Pulse Tailoring with UV Laser Source Improves Throughput and Quality for High-Density Packaging Glass Interposer Drilling

Jim BOVATSEK[*1], Rajesh PATEL[1], Philipp VON WITZENDORFF[2], Andrea BORDINA[2], Oliver SUTTMANN[2], Ludger OVERMEYER[2]

[*1] *Spectra-Physics, 3635 Peterson Way, Santa Clara, CA 95054, United States of America*
E-mail: jim.bovatsek@spectra-physics.com
[2] *Laser Zentrum Hanover e.V., Hollerithallee 8, 30419 Hanover, Germany,*

Glasses of various types and thicknesses are finding increasing application in a variety of markets. For smartphones and other portable electronic devices, chemically-strengthened aluminosilicate glasses are used as a strong protective cover glass over the display panel. For interposers used in chip-scale packaging, manufacturers are increasingly using very thin borosilicate and alkali-free glasses. In both cases, manufacturers are looking to laser processing technologies to provide the required quality and throughput. For very good quality machining, lasers with pico- and femtosecond pulse durations may be used; however it may not be possible to meet challenging throughput and cost requirements. Besides short pulse durations, shorter wavelengths can also be beneficial. Recently, a high power 355 nm nanosecond laser was developed which allows for pulse width and shape tailoring in the time domain. A virtually limitless flexibility in pulse duration, pulse shape, pulse multiplicity, and pulse repetition frequency is possible, thus opening up an entire new processing space not possible with conventional Q-switched nanosecond laser technology. In this work, various glasses are processed and analysis is performed with respect to both throughput and quality. The effect of varying pulse duration from 2 – 10 ns is characterized and the impact of processing with multiple "burst" pulses is also studied.

Keywords: UV laser, glass processing, HDI, PCB, interposer, drilling

1. Introduction

Laser processing of glass and other transparent brittle materials is of increasing importance for the manufacturing of a wide range of products we use on a daily basis. For touch panel displays on mobile devices, lasers have shown themselves as capable tools for cutting chemically strengthened glass [1] with both high speed and good quality. Some researchers have characterized the machining capability of ns pulses with different wavelengths on u-strengthened borosilicate glass [2]. For the LED lighting industry, lasers have been a valuable tool over the years for device singulation on the sapphire substrate [3]. Currently, glass is increasingly considered as an interposer material for advanced high density IC packaging architectures, and lasers are being considered as a tool for drilling the through-glass vias (TGVs) required for lead connections [4].

Recently, researchers from Spectra-Physics' industrial application laboratory collaborated with Laser Zentrum Hannover (LZH) located in Hannover, Germany on a series of experiments aimed at developing high-quality and high-throughput process for drilling thin glass plates using a state-of-the-art nanosecond pulse diode-pumped solid state laser (DPSS) operating at the 355 nm ultraviolet (UV) wavelength. Initial experiments were performed to determine the fundamental effect of various laser parameters on glass ablation depth and quality. The results were then used to develop processing for drilling through-glass vias (TGVs) in ultra-thin (50 µm) glass as well as micro-TGVs in somewhat thicker (200 µm) glass

1.1 Quasar laser

All work was executed using a Spectra-Physics' Quasar® 355-60 pulsed UV laser, which has a novel temporal pulse tailoring feature known as TimeShift™ technology. This allows a single laser to output a wide variety of pulse types – from short (<2 ns) to long (>100 ns) pulse width, stand-alone or burst configuration, and with pulse burst separation times from <5 ns to greater than 200 ns. Fig. 1 shows a photograph of the Quasar laser.

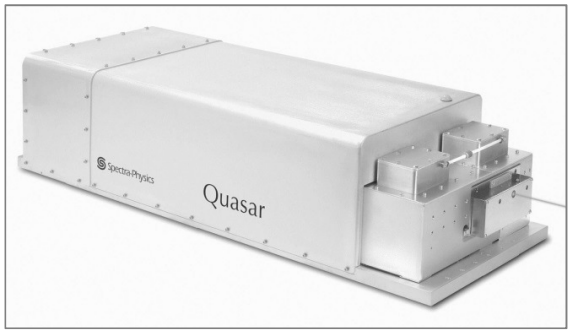

Fig. 1 Photograph of Quasar UV laser with TimeShift technology.

Besides pulse width adjustability, TimeShift technology can also be used to customize the shapes of individual

pulses as well as the envelope containing a burst of pulses (i.e. tailor the relative intensity of pulses in a burst). In short, complete pulse tailoring in time is possible with TimeShift.

2. Single line scan experiments

In these experiments, single line scans at various scan speeds were used to scribe grooves in 400 µm thick Schott D-263 borosilicate glass. The machining depth and edge chipping dimension were characterized for each of the features. The goal of this test was to check for a fundamental difference in processing speed and quality for the various pulse outputs.

2.1 Experimental setup, parameters, and procedures

Single line scan features were generated using a 2-axis scanning galvanometer head directing the beam through an f-theta objective and on to the work piece. The focal length was 100 mm and the calculated focal beam diameter at the workpiece was 15 µm, $1/e^2$. Scanning speeds were adjusted so as to generate spot overlaps on the material in the range of 20-80%. The pulse overlap (O_p) is here defined based on the optical focus spot diameter ($2w_o$) and relates to the scan speed (Vs) and laser pulse repetition frequency (PRF) according to the equation:

$$O_p = 1 - \frac{Vs}{2w_o \times PRF} \qquad (1)$$

From equation (1), it is clear that for the same pulse overlap, operation at a different PRF will necessarily require a proportionate adjustment to the scan speed.

The values and ranges of process parameters used for the tests are listed in Table 1.

Table 1 Parameters used in single line scan experiments

Parameter	Units	Values
Pulse width	ns	2, 5, 10, 2×10
Fluence	J/cm^2	27 – 90
Pulse overlap	%	20 – 80
Repetition rate	kHz	100, 200

For the case of the 2×10 ns burst mode output, there is an additional parameter space to optimize. Similar to a study performed by Javaux Léger et al. [5], the pulse separation time was varied (5 – 200 ns in this work). In addition, the relative intensity of the two pulses was varied as (1) a 1:1 ratio, with equal intensity for both pulses, (2) a 2:1 ratio with a doubled intensity in the first pulse, and (3) a 1:2 ratio with a doubled intensity in the second pulse. Fig. 2 shows photodiode oscilloscope traces of the double pulse output and illustrates the parameters that were adjusted.

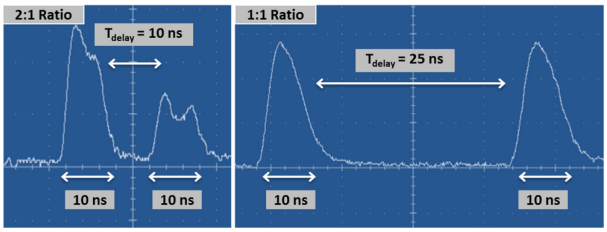

Fig. 2 Photodiode pulse traces showing additional parameters for the 2×10 ns pulse output mode.

Ablation depth and edge chipping were measured with optical microscopy. Measurements were made at three different locations along the length of each scribed line. At each of the three measurement locations, two distinct width measurements were made: the maximum ablation width b_{max}, which includes the maximum extent of chipping on both sides of the trench, and the minimum ablation width b_{min}, which corresponds to the expected deterministic ablation kerf width. The chipping dimension, $b_{chipping}$, is defined in equation (2) below:

$$b_{chipping} = \frac{b_{max} - b_{min}}{2} \qquad (2)$$

The graphic in Fig. 3 depicts a top-down view of a laser scribe and illustrates how $b_{chipping}$ is defined.

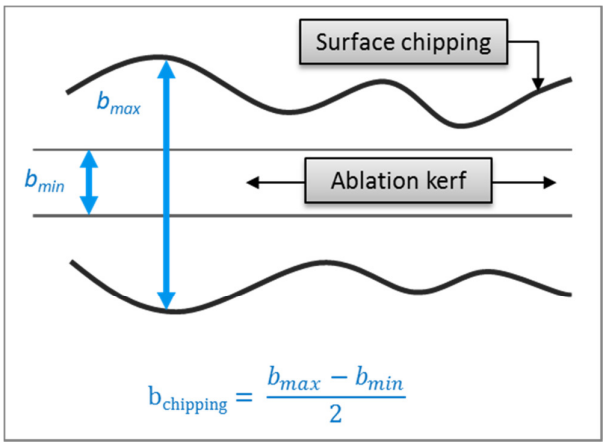

Fig. 3 Illustration showing how edge chipping is defined.

2.2 Results and discussion

The ablation depth for the single pulse output and the double 10 ns pulse output are plotted vs. pulse overlap in Fig. 4 below. As expected, the ablation depth increases with increasing overlap for all pulse outputs, since the correspondingly lower speed, at the same PRF, results in more pulses irradiating the material for a given duration. For the single pulse output, the 10 ns pulse width generates deeper scribes than both the 2 ns and 5 ns outputs, which have similar depths. For the 2×10 ns output, there is a very strong depth advantage compared to the single 10 ns pulse output. In addition, the 1:2 and 2:1 intensity distributions generate significantly deeper scribes compared to the 1:1 distribution.

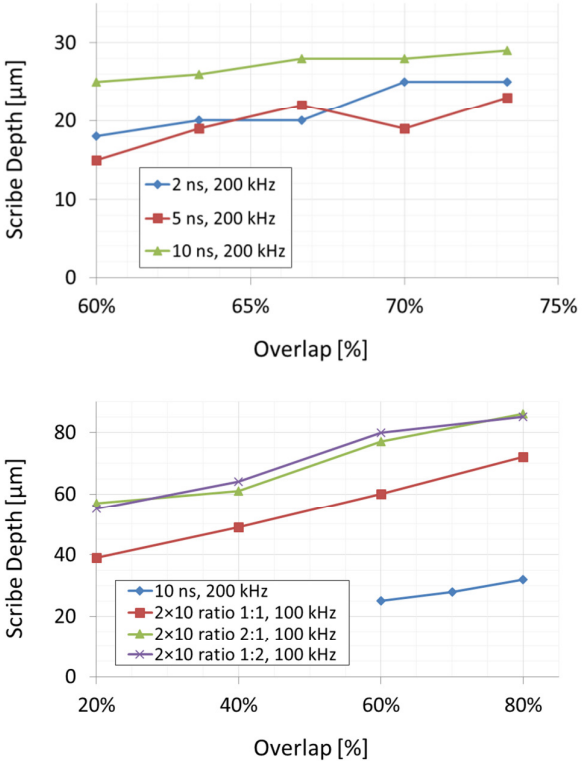

Fig. 4 Depth vs. overlap for single pulse output (top), and 2×10ns double pulse output (bottom).

It is important to point out that for the 2×10 ns pulse output, which is operated at 100 kHz (compared to 200 kHz for single 10 ns pulse), the scanning speed at a particular overlap is half that of the single 10 ns pulse output, in accordance with the definition of pulse overlap in equation (1). However, even when considering this, there is still a very strong depth advantage with the double pulse output. For example, the single 10 ns pulse depth at 80% overlap (600 mm/s scan speed) is barely 40% the depth for the double pulses at the same scan speed (60% overlap for the 100 kHz PRF).

The edge chipping data for the single pulse output are plotted vs. pulse overlap in Fig. 5. At the bottom of Fig. 5 are optical micrographs of the scribes for the 10, 5, and 2 ns pulse durations. The data indicates a large decrease in edge chipping when going from 5 to 2 ns pulse duration.

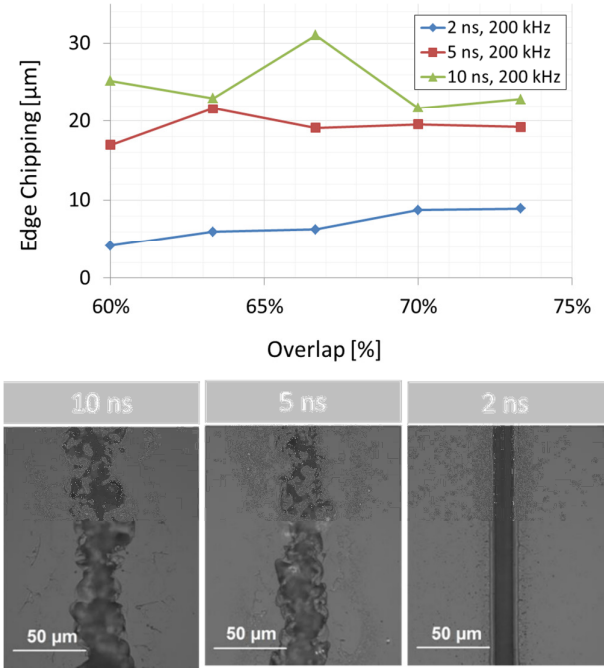

Fig. 5 Edge chipping vs. overlap (top), and optical microscope photos (bottom) for the three pulse durations.

From the data plot, the chipping for 2 ns pulse width is less than half that for 5 ns. This is somewhat surprising considering the ablation depths are similar for the two pulse widths (see data in Fig. 4). The edge chipping difference is strongly evident in the microscope photos, with the edge quality at 2 ns being significantly improved over that of the 5 and 10 ns pulse durations. This large improvement in edge quality with 2 ns pulse width may indicate a different material removal mechanism is at work compared to the longer pulse widths, something closer to direct ablation as opposed to thermal shock and fracture.

Edge chipping was also analyzed for the 2×10 ns pulse output for different intensity ratios. This data, in Fig. 6, shows that the intensity distribution between the pulses does in fact have an impact on the quality.

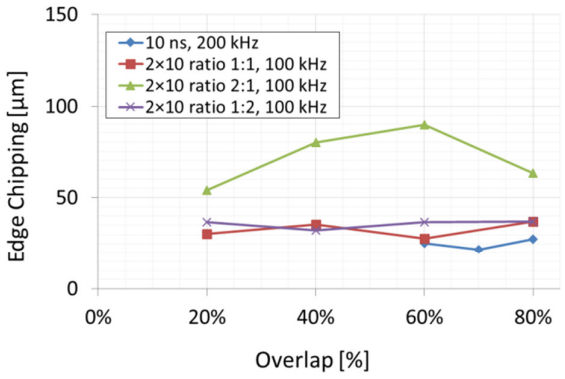

Fig. 6 Edge chipping for different relative intensity of 2×10 ns pulse output compared to a single 10 ns pulse.

Fig. 6 shows a clear disadvantage when processing with a higher intensity first pulse in the double pulse output mode, particularly in the middle range of pulse overlaps. The reason for this is not clear, but it may be due to more thermal shock with the leading first pulse having higher intensity. In contrast, the lower intensity first pulse for the 1:1 and 1:2 cases may have the effect of pre-heating the material and so there is less thermal shock with the follow-up pulse.

An additional test using the 1:1 double pulse intensity ratio was performed in order to characterize the ablation depth for a variety of pulse separation times, ranging from 5 to 200 ns. For the range of overlaps tested, 20-80%, the shortest pulse separation of 5 ns resulted in the deepest ablation, followed very closely by the 10 ns separation, which was typically 10% lower in ablation depth. All other separation times (25, 50, 100, 200 ns) were clustered together at approximately 2/3 the depth of the 5 ns separation.

3. Fabrication of through glass vias in ultra-thin glass

The results from the single line scan ablation experiments were used to guide a specific process development effort: trepan-drilling a TGV in ultra-thin glass. The material was 50 µm thick Schott D263 borosilicate glass and the target via diameter was 500 µm. The trepanning speed for the small diameter was kept in the range of 50-100 mm/s and to avoid excessive heat accumulation in the glass, the laser was operated in the range 5-10 kHz, resulting in a fixed pulse overlap of 67%.

The quality and throughput of the vias processed with the various TimeShift pulse outputs were consistent with results from the single line scan experiments. Using a single 2 ns pulse output, the quality was good but the throughput was relatively low. Likewise, using a 2×10 ns with 1:2 intensity ratio pulse output resulted in lower quality TGVs but at a much higher processing rate. Using just a single 10 ns pulse duration, the quality was similar to the double pulse output but with just half the throughput. In an attempt to combine the best quality result with the highest throughput result, a TGV was also fabricated using a two-step process: an initial "ground-breaking" process with 2 ns pulses to establish good edge quality, followed by higher throughput ablation with the 2×10 ns output. Fig. 7 below summarizes the results with optical micrographs and tabulated data for select TGV drilling processes.

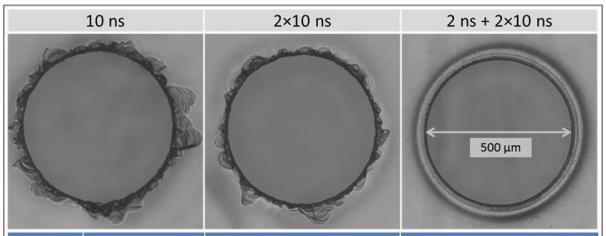

Pulse Pattern	10 ns	2×10 ns	2 ns + 2×10 ns
Chipping Size	80 µm	73 µm	20 µm
Drill Time	0.31 s	0.13 s	0.14 s
Process Fluence	62 J/cm²	90 J/cm²	36 J/cm² + 90 J/cm²

Fig. 7 Summary of TGVs drilled with various pulse outputs.

From Fig. 7, it is clear that the hybrid, 2-step process generated the desired result. With nearly the same process time as the high throughput 2×10 ns process, the excellent edge quality of the single 2 ns pulse output is achieved. In this case, the commonly encountered need to compromise speed for quality—or vice-versa—was avoided by careful application of the Quasar laser's flexible TimeShift pulse tailoring technology.

4. Fabrication of low taper micro through glass vias

When machining relatively large features in very thin glass, such as the 500 µm diameter vias in the 50 µm thick glass from the previous result, excessive sidewall taper of the via is not challenging to avoid. The aspect ratio of the feature, which is commonly defined as the ratio of the material thickness to the via diameter, was quite small at 50 µm / 500 µm, or 1:10. Laser processing of larger aspect ratio features in materials is more challenging, for various reasons: there can be shadowing effects which attenuate the beam as it propagates through the deep feature, the ablation debris may not have sufficient energy to eject out of the deep via and thus have a clogging effect, and there can be diffractive spreading of the beam, resulting in decreased energy density, if the Rayleigh range of the focused beam is small relative to the material thickness.

For glass interposers used in high-density interconnect (HDI) printed circuit board (PCB) packaging, however, the glass plate is typically thicker (100-300 µm) and the target via diameters are much smaller (10-50 µm diameter), which mandates the need to machine TGVs with significantly higher aspect ratios, ranging from 2:1 on the low side up to 30:1 on the high side. To assist in machining low-, no-, or reverse-taper vias in materials, various optical systems have been developed which trepan a focused laser beam in a target material and in addition offer, to some extent, independent control of the angle and offset of the focused beam relative to the axis of rotation axis.

4.1 Equipment and parameters

In this work, low taper micro-TGVs were machined in 200 µm thick alkali-free borosilicate glass. Using the Quasar 355-60 laser system a custom built beam trepanning system (HAAS Laser Technologies, Inc.), TGVs with small diameters of ~25-35 µm and relatively low sidewall taper were drilled in the glass. Table 2 contains a list of the parameters used for the tests.

Table 2 Parameters used in micro-TGV experiments

Parameter	Values
Pulse width	2 ns
Focal diameter	Ø 8 µm, $1/e^2$
Repetition rate	2.5 – 50 kHz
Pulse energy	60 µJ
Trepan speed	1000 rotations per minute (RPM)
Time per trepan revolution	60 ms
Beam precession angle	25°
Material	Schott AF45 alkali-free borosilicate glass, 200 µm thick

In this first test with the trepanning head, only the single 2 ns pulse output of the Quasar was tested. This was desired in order to set a baseline for the best quality that can be achieved amongst the numerous pulse outputs of the Quasar laser. In fact, all other pulse outputs used in the single line scan experiments resulted in edge chipping either similar in size and in many cases larger than the target diameter of the micro-vias.

Vias were fabricated by setting the trepanning motor in motion at a rotation speed of 1,000 rotations per minute (RPM) and firing the laser pulses until a predefined number of trepan revolutions had completed. Only complete trepan revolutions were allowed in the parametric tests, and therefore all exposure times were integer multiples of the time required for a single revolution, 60 ms.

4.2 Effect of pulse repetition frequency

The Quasar laser is capable of a wide range of pulse repetition frequencies (PRFs)—from single shot operation up to several MHz. For focusing in thin brittle materials, it is important to determine the highest PRF that can be used before the onset of detrimental thermal effects (such as melting, chipping, and cracking) occurs. Initial analysis was aimed at detecting lateral micro-cracking when viewing the top surface of ablated vias with an optical microscope. Fig. 8 shows a sequence of optical microscope photos of vias drilled at increasing PRFs.

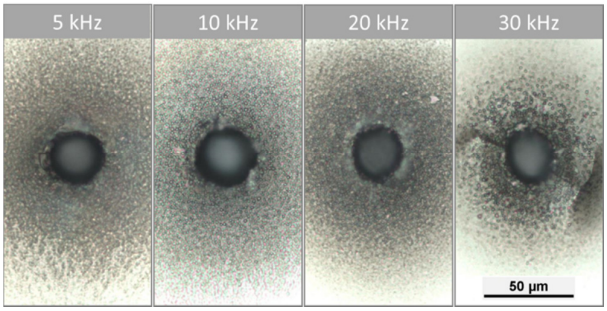

Fig. 8 Optical microscope photos of entry surfaces of TGVs drilled with 6,000 pulses at 5-30 kHz PRF.

For all PRFs the same number of pulses (6,000) were used to drill the vias; consequently, the higher PRFs required less time to drill (in proportion to the inverse of the PRF value). With the same cumulative energy input to the work piece in shorter time, there is the potential for a corresponding increase in thermal loading, which might be detrimental to the quality of the vias. From 5 up to 20 kHz, the surface quality appears quite similar with no cracking evident; however from 20 to 30 kHz, the onset of severe micro-cracking is observed. For the lower PRFs where micro-cracking is not observed, the edge chipping appears quite small as expected for the 2 ns pulse duration, based on the previous single line scan result.

4.3 Sidewall taper evolution

Additional processing and analysis were undertaken for vias drilled using a PRF of 5 kHz, deemed low enough to assure that no detrimental heat accumulation was impacting the results. To characterize the evolution of the sidewall angle, vias were drilled with a low to high number of trepan revolutions, and the entry and exit hole diameters were measured. Knowing the entry and exit diameters, D_{ent} and D_{ext} respectively, and the glass thickness T_{glass}, the sidewall angle, θ_s, is calculated according to equation (3) below:

$$\tan\theta_s = 0.5 \times \left(\frac{D_{ent}-D_{ext}}{T_{glass}}\right) \qquad (3)$$

From equation (3), the sidewall angle is defined as the angular deviation from the case of perfect perpendicularity with respect to the glass surface. Hence, a value of zero implies there is no angular taper and the entry and exit diameters are equal. The diameter data, along with a calculated sidewall angle as a function of trepan revolutions, are plotted in Fig. 9.

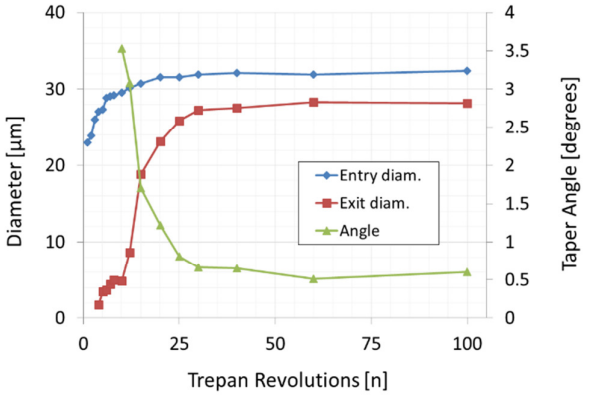

Fig. 9 Data plot showing entry and exit diameters and sidewall taper angle with increasing trepan revolutions.

Fig. 9 shows that beginning at ~5 revolutions, there is a very small but measurable exit diameter, signifying the transition of the drill feature from a blind via to a through via. In the span from about 10 to 25 revolutions, the exit diameter rapidly grows to within about 75% of the entry diameter. Beyond 25 revolutions, the exit diameter grows towards an asymptotic maximum of about 28 µm, which is 87.5% of the maximum entry diameter of 32 µm. Considering the average via diameter as (32+28)/2 = 30 µm, the aspect ratio of the trepanned via is about 6.5:1, which is somewhat large for a low/no taper ablation feature. It is also noteworthy that at 25 revolutions and beyond, the taper angle decreases to below 1 degree, which equates to a sidewall angle of >89º.

The cross-sectional geometry of the features measured in Fig. 9 was also analyzed via optical microscopy, with optical microscope photographs displayed in Fig. 10. The images show how the geometry of the vias evolves with increasing trepan revolutions.

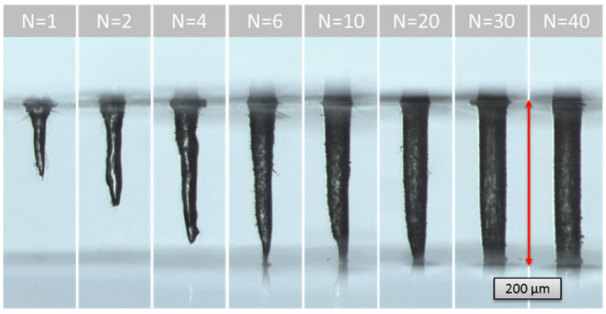

Fig. 10 Optical microscope photos showing micro-TGV evolution with increasing trepan revolutions (N).

The sidewall taper evident in the cross-sectional views of the vias are somewhat consistent with the taper angle calculated based on the measurements of the entry and exit diameters from Fig. 9. However, there is also a tendency for the sidewalls to have less taper near the entry surface and through much of the bulk material, before steeply closing in to generate a small exit diameter. Therefore, calculating taper angles based simply on the entry and exit diameters is less predictive of the overall sidewall geometry for the case of few trepan revolutions; however, for >25 revolutions the via is ablated nearly to saturation and the taper angle calculation is very consistent with the observed sidewall geometry.

5. Conclusion

A Spectra-Physics Quasar 355-60 laser with TimeShift pulse shaping technology has been tested for ablation of borosilicate glass used in microelectronics packaging applications. Comprehensive single line scan experiments in D263 borosilicate glass demonstrated that the 2 ns short pulse output can offer very good ablation quality while the 2×10 ns double pulse output with 2:1 intensity ratio has unexpectedly high ablation rates that are ~2.4× that of a single 10 ns pulse while maintaining the same edge quality. A hybrid process was developed for TGV trepan-drilling in ultra-thin 50 µm thick D263 borosilicate glass. By starting off the process with a single 2 ns pulse width and following with a 2×10 ns double pulse output, a high throughput and high quality TGV was realized, representing a best of both worlds scenario in which speed did not have to be sacrificed for quality, and vice-versa. For micro-TGV drilling in a slightly thicker glass (200 µm), a taper control beam trepanning module was used to generate good quality, low taper vias for HDI packaging interposer application, with the 2 ns pulse output resulting in very small surface chipping from 0-10 µm. Throughout the series of experiments, the ability to tailor both quality and throughput with the Quasar's TimeShift pulse-shaping technology was clearly evident, and the ability of a hybrid process using multiple pulse output profiles to realize both best quality and highest throughput was clearly demonstrated.

References

[1] A. Abramov, M. Black, and G. Scott Glaesemann: Physics Procedia, 5-b, (2010) p.285.

[2] S. Nikumb, Q. Chen, C. Li, H. Reshef, H.Y. Zheng, H. Qiu, and D. Low: Thin Solid Films, 47, (2005), p.216.

[3] E. Rea, Jr.: Proc. SPIE 5339, Photon Processing in Microelectronics and Photonics III, San Jose, (2004) p.231.

[4] M. Töpper, I. Ndip, R. Erxleben, L. Brusberg, N. Nissen, H. Schröder, H. Yamamoto, G. Todt, and H. Reichl: Proc. Electronic Components and Technology Conference, Las Vegas, (2010) p. 66.

[5] C. Javaux Léger, K. Mishchik, O. Dematteo-Caulier, S. Skupin, B. Chimier, G. Duchateau, A. Bourgeade, C. Hoenninger, E. Mottay, J. Lopez, and R. Kling: Proc. SPIE 9351, Laser-based Micro- and Nanoprocessing IX, San Francisco, (2015) p.93510M.